BUTTERWORTH HEINEMANN

Polymer Vol. 36 No. 19, pp. 3633–3639, 1995
Copyright © 1995 Elsevier Science Ltd
Printed in Great Britain. All rights reserved
0032-3861/95/$10.00+0.00

Supermolecular structure of oriented and semicrystalline poly(ethylene terephthalate) as revealed by the electron density correlation function from small-angle X-ray scattering studies

U. Göschel*† and G. Urban
Max-Planck-Institut für Polymerforschung, Postfach 3148, D-55021 Mainz, Germany
(Received 7 April 1994; revised 7 February 1995)

Small-angle X-ray scattering (SAXS) is employed to study the supermolecular structure of uniaxially oriented and semicrystalline poly(ethylene terephthalate) (PET) samples. By means of a multistep zone drawing procedure carried out at different temperatures and loading conditions an extraordinarily high chain orientation is achieved. Using the electron density correlation function obtained from the Fourier transformed experimental scattering intensity, structure parameters such as the most probable long period, the average lamellar thickness, and the volume crystallinity are determined. By obtaining these parameters from only one experiment one can neglect possible effects from a combination of methods and thus gain new insights into the structure formation process under drawing.

(Keywords: small-angle X-ray scattering; oriented lamellar structures; poly(ethylene terephthalate))

INTRODUCTION

Small-angle X-ray scattering (SAXS) techniques have been widely used to investigate the lamellar structure of semicrystalline polymers[1–3]. Assuming a periodic two-phase lamellar system, Vonk and Kortleve[4,5] found that the electron density correlation function obtained from the Fourier transformed scattering intensity can provide detailed information about the supermolecular structure. In 1980, Strobl and coworkers[6,7] investigated the general properties of the electron density correlation function of isotropic and semicrystalline polymers with a lamellar structure. Their work revealed that the correlation function immediately provides the following structure parameters: the most probable long period, the average lamellar thickness, the volume crystallinity, the specific inner surface, and, if the scattering intensities are measured in absolute values[2,3], the electron density difference between the crystalline and amorphous regions.

Zachmann and coworkers[8] investigated the supermolecular structure of isothermally crystallized poly(ethylene terephthalate) (PET) by means of the electron density correlation function as well as the interface distribution function. They reported that the long period obtained by simply applying Bragg's law is considerably larger than the true value. Furthermore, the distributions of the crystal thickness and the long period were both found to be very broad.

The electron density correlation function was applied to anisotropic structures by various researchers, including Bonart[9], Dettenmaier[10], and Stribeck and coworkers[11–13]. In the case of two-dimensional SAXS patterns with a cylindrical symmetry, i.e. usually in the fibre direction, the one-dimensional electron density correlation function can be calculated and used to describe the variation of the electron density along the fibril or the height of a lamellar stack.

In this present paper the experimental SAXS data from uniaxially oriented and semicrystalline PET samples, discussed in ref. 14, will be analysed by means of the one-dimensional electron density correlation function, $K(x_3)$, along the orientation direction, x_3. A zone drawing procedure with several steps[15] is used to achieve the desired anisotropic structures[16,17]. According to wide-angle X-ray scattering (WAXS) experiments[17] the crystallite orientation is extraordinarily large. Previous SAXS studies on the PET samples referred to above[14] revealed a lamellar structure with a scattering intensity distribution symmetrical to the meridian, b_3, where the scattering vector component, b_3 is parallel to x_3 (see *Figure 1*).

The one-dimensional electron density correlation function, $K(x_3)$, is calculated from two-dimensional scattering patterns using a Nicolet area detector. The experimental scattering intensities are then projected on to the meridian, b_3. The structural parameters derived from $K(x_3)$ are discussed for several PET samples which were obtained by using different drawing conditions. The possibility of obtaining structural information about the long period, lamellar thickness, and volume crystallinity

* To whom correspondence should be addressed
† Present address: Department of Material Systems Engineering, Tokyo University of Agriculture and Technology, Koganei, Tokyo 184, Japan

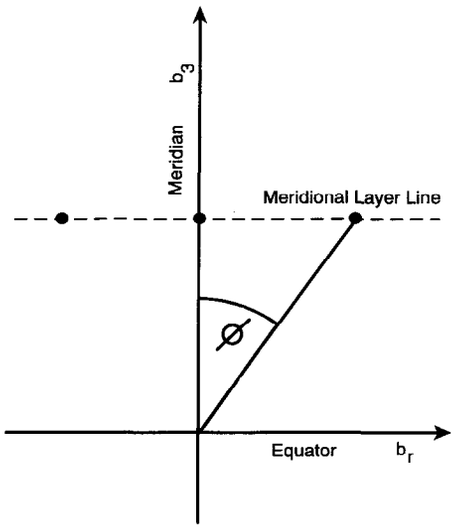

Figure 1 Coordinate system in reciprocal space

from only one experiment is advantageous because of the absence of possible effects from using a combination of methods and will provide new insights into the structure formation under drawing. Furthermore, this present paper contributes generally to the treatment of SAXS data of oriented polymer structures.

Theoretical background

The experimental scattering intensity, $I(\boldsymbol{b})$, arising from the electron density difference:

$$\eta(\boldsymbol{x}) = \rho_{el}(\boldsymbol{x}) - \langle \rho_{el}(\boldsymbol{x}) \rangle \tag{1}$$

where the brackets $\langle\ \rangle$ denote the average over the irradiated volume V, is given by the following:

$$I(\boldsymbol{b}) = |A(\boldsymbol{b})|^2 = \left| \iiint_V \eta(\boldsymbol{x}) \exp(-2\pi i \boldsymbol{b}\boldsymbol{x})\, d\boldsymbol{x} \right|^2 \tag{2}$$

or

$$I(\boldsymbol{b}) = \iiint_V \tilde{\eta}(\boldsymbol{x}) \exp(-2\pi i \boldsymbol{b}\boldsymbol{x})\, d\boldsymbol{x} \tag{3}$$

In this expression $\tilde{\eta}(\boldsymbol{x})$ is the self-convolution or auto-correlation of $\eta(\boldsymbol{x})$:

$$\tilde{\eta}(\boldsymbol{x}) = \iiint_V \eta(\boldsymbol{x}+\boldsymbol{y})\eta(\boldsymbol{y})\, d\boldsymbol{y} \tag{4}$$

$A(\boldsymbol{b})$ is the scattering amplitude and $\boldsymbol{b}$ the scattering vector, given by the following:

$$b = |\boldsymbol{b}| = \frac{2\sin\theta}{\lambda} \tag{5}$$

where 2θ is the scattering angle and λ is the wavelength of the radiation. The vectors $\boldsymbol{x}$ and $\boldsymbol{y}$ and their components x_1, x_2, x_3 and y_1, y_2, y_3, respectively are defined in physical space.

Let us now introduce the electron density correlation function[10]; which is given by the following:

$$K(\boldsymbol{x}) = \frac{\tilde{\eta}(\boldsymbol{x})}{\tilde{\eta}(0)} = \frac{\tilde{\eta}(\boldsymbol{x})}{V\langle \eta^2 \rangle} \tag{6}$$

which is normalized at the origin, i.e. $K(0) = 1$.

Then, according to equations (2) and (6) the scattering

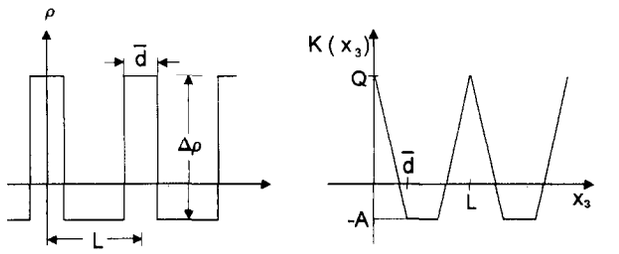

Figure 2 Electron density distribution, $\rho(x_3)$, and the related correlation function, $K(x_3)$, for a lamellar system with an idealized periodic two-phase regularity

intensity is given by the three-dimensional Fourier integral:

$$I(\boldsymbol{b}) = V\langle \eta^2 \rangle \iiint_V K(\boldsymbol{x}) \exp(-2\pi i \boldsymbol{b}\boldsymbol{x})\, d\boldsymbol{x} \tag{7}$$

and the inverse Fourier transformation yields the following:

$$K(\boldsymbol{x}) = (V\langle \eta^2 \rangle)^{-1} \iiint_V I(\boldsymbol{b}) \exp(2\pi i \boldsymbol{b}\boldsymbol{x})\, d\boldsymbol{b} \tag{8}$$

With respect to equations (2) and (6) the electron density correlation function, $K(\boldsymbol{x})$, describes the probability of finding an electron density fluctuation, $\eta(\boldsymbol{x})$, at the point $\boldsymbol{x}$ in relation to the fluctuation $\eta(0)$ at the origin[10].

Now, we can suppose cylindrical symmetry regarding the x_3 component and define x_3 as the drawing direction where the resulting intensity function $I(\boldsymbol{b})$ is cylindrically symmetrical to the scattering component in reciprocal space, b_3 (*Figure 1*). We can then write the following:

$$I(\boldsymbol{b}) = I(b_r, b_3) \tag{9}$$

where b_r denotes the radial component of the scattering vector with:

$$b_r = \sqrt{b_1^2 + b_2^2} \tag{10}$$

and the axial components b_1 and b_2.

With regard to equation (8) the one-dimensional electron density correlation function can be written in the following form:

$$K(0,0,x_3) \approx \int_0^\infty I_L(b_3) \cos(2\pi b_3 x_3)\, db_3 \tag{11}$$

where the intensity function along the meridian, $I_L(b_3)$, is given as follows:

$$I_L(b_3) = 2\pi \int_0^\infty b_r I(b_r, b_3)\, db_r \tag{12}$$

In equation (11) various structure-independent correction factors[3], such as the Thomson, polarization, and Lorentz factors are neglected.

Assuming a periodic density distribution, with a lamellar structure consisting of alternately arranged crystalline and noncrystalline phases with a crystallinity lower than 0.5, the resulting one-dimensional electron density correlation function, $K(x_3)$, for such an idealized two-phase structure can be represented, according to Strobl and Schneider[6], as shown in *Figure 2*. The crystalline lamellae are characterized by an average thickness, $\bar{d}$, and an average density, ρ_c, separated by a

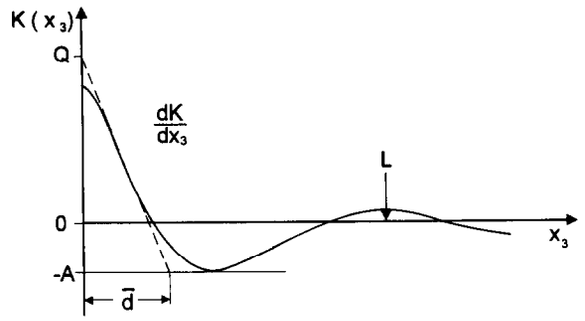

Figure 3 One-dimensional electron density correlation function, $K(x_3)$, and general properties of $K(x_3)$ for a lamellar two-phase system with regularities of real polymer structures

noncrystalline phase with an average density, ρ_a. In real polymer systems the interlamellar and lamellar thicknesses can vary, and, in addition, the phase boundaries are not sharp. This is why the $K(x_3)$ functions for real systems are similar to the correlation function which is represented in *Figure 3*. With deviation from the idealized structure, $K(x_3)$ changes from triangles of constant amplitude into aperiodic sinusoidal curves. According to Strobl *et al.*[7], the following essential lamellar structure parameters can be determined from the calculated $K(x_3)$. The average lamellar thickness, $\bar{d}$, is given by the intersection of the extrapolated straight line dK/dx_3 on the enveloped 'self-correlation triangle' at low values of x_3 and the 'baseline' at $-A$. Here, the 'baseline' means a straight line parallel to the abscissa, x_3, cutting the first $K(x_3)$ minimum which belongs to the 'self-correlation triangle' (*Figure 3*). The volume crystallinity, w_c, is defined by the following:

$$w_c = A/(A + Q) \tag{13}$$

where $-A$ and Q denote the intersection of $K(x_3 = 0)$ with the 'base line' and the extrapolated straight line dK/dx_3 inside the 'self-correlation triangle', respectively. The most probable long period, L, corresponds to the x_3 value which belongs to the first $K(x_3)$ maximum outside the 'self-correlation triangle'.

EXPERIMENTAL

Sample preparation

Poly(ethylene terephthalate) (PET), with a molecular weight, $M_w = 20\,000$, was uniaxially drawn under well defined conditions in order to achieve the desired anisotropic structures. Starting from an isotropic ($\Delta n = 0.5 \times 10^{-3}$) and noncrystalline structure (according to WAXS), a multistep zone drawing procedure was used to obtain semicrystalline structures with an extraordinarily large chain orientation. The drawing procedure, described by us in ref. 15, was performed over the temperature range from room temperature to 230°C, and with a drawing stress ranging from 15 to 400 MPa (*Table 1*). Applying these conditions, a draw ratio from 5.4 to 7.3, a birefringence from 0.202 to 0.249, and an elastic modulus from 12.0 to 16.8 GPa were achieved. The sample designation in this present paper is taken from those found in refs 14–17.

SAXS experiment

Small-angle X-ray scattering (SAXS) experiments were carried out with CuKα radiation, provided by a 18 kW rotating anode X-ray source (Rigaku RV-300). The radiation was Ni-filtered, monochromaticized, and point collimated with a beam diameter of ~ 1.0 mm. The SAXS intensity was measured by using a Nicolet area detector. With respect to the distance of 890 mm between sample and detector and a laminated sample thickness of ~ 300 μm the irradiation time was fixed at 65 h. Standard procedures were used for correction of the detector sensitivity, primary beam profile, and background.

Determination of the correlation function

Starting from the two-dimensional SAXS patterns with a scattering intensity distribution symmetrical to the meridian, the measured intensity, $I(b_r, b_3)$, was projected on to the b_3-axis corresponding to the drawing direction, x_3, (*Figure 1*) by means of the following:

$$I_L(b_3) = \sum_{n=1}^{512} 2\pi b_{r,n} I(b_r, b_3) \Delta b_{r,n} \tag{14}$$

where n is the number of channels ranging from 1 to 512 which cover the scattering patterns.

Because of the integral limits in equation (11) one must know the entire small-angle X-ray scattering curve $I_L(b_3)$. This means that $I_L(b_3)$ has to be extrapolated to $b_3 \to 0$ and $b_3 \to \infty$. In the case of $b_3 \to 0$ the experimental $I_L(b_3)$ curve was extrapolated by a straight line. According to Vonk and Kortleve[4] such an extrapolation has only a very small effect on the relevant part of the correlation function. Neither the position nor the height of the first maximum should be seriously influenced.

The tail of the scattering curve $I_L(b_3)$ at large b_3 values was extrapolated to $b_3 \to \infty$ by means of Porod's law[18]:

$$\lim_{b_3 \to \infty} I_L(b_3) = \frac{B}{b_3^4} + U \tag{15}$$

Table 1 Drawing parameters and characterization of the structural anisotropy

Sample	Maximum drawing temperature T (°C)	Maximum drawing stress σ_{max} (MPa)	Maximum draw ratio λ	Birefringence Δn	Elastic modulus E (GPa)
2	160	350	6.3	0.202	13.4
3	200	385	7.1	0.228	15.0
4	230	400	7.3	0.205	16.8
5	200	400	7.2	0.249	14.3
9	180	100	5.4	0.219	12.0

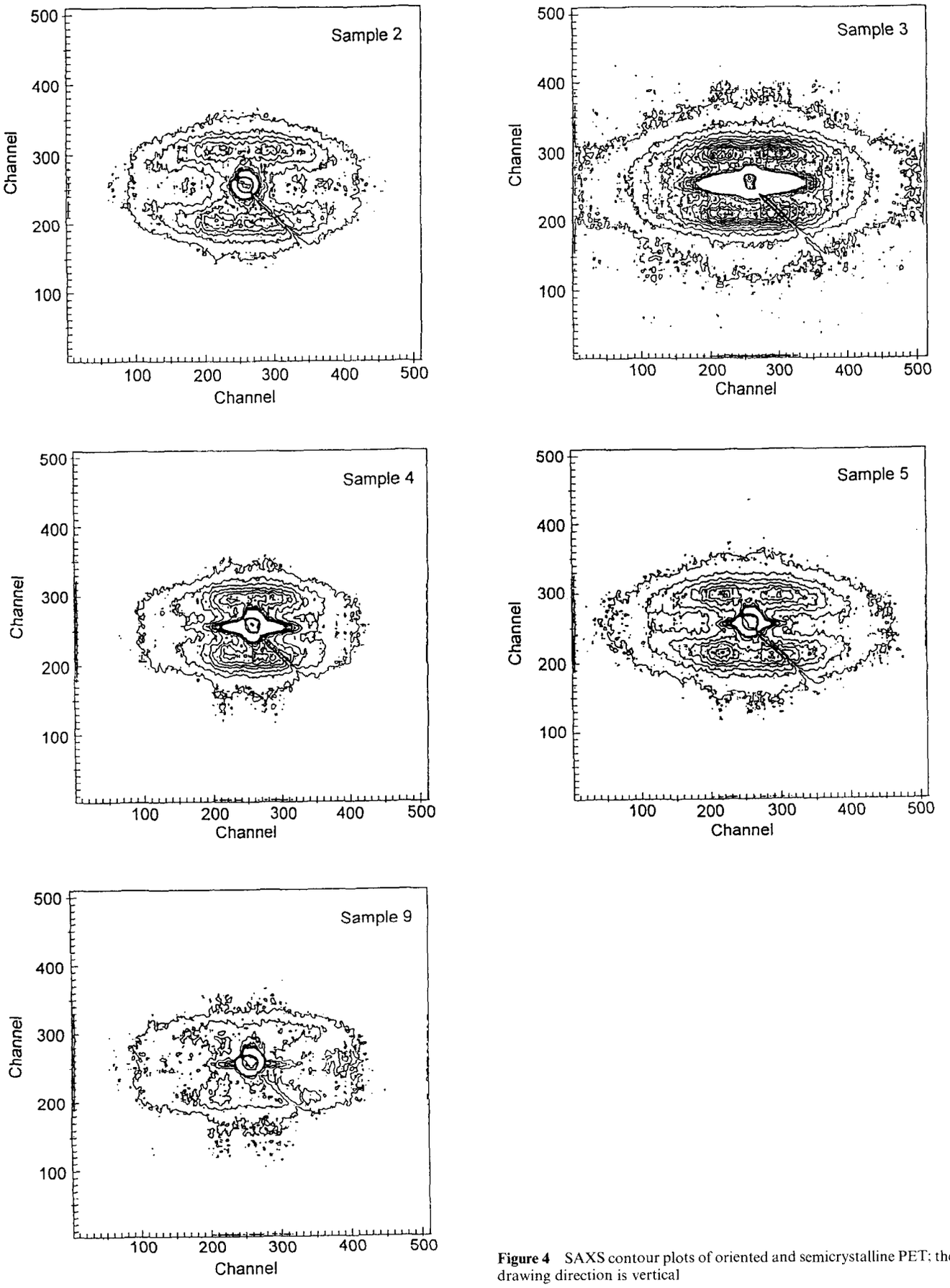

Figure 4 SAXS contour plots of oriented and semicrystalline PET; the drawing direction is vertical

where B is a constant and U the scattering background. Porod's law is valid for a two-phase system with sharp boundaries. A real polymer structure will differ to either a lesser or a greater extent from this idealized assumption, but it can be shown that the correlation function is seriously affected only at small b_3 values[4].

RESULTS AND DISCUSSION

Figure 4 represents the two-dimensional SAXS patterns of the differently prepared PET samples 2–5 and 9. The supermolecular structure was previously discussed by us in detail in ref. 14. Depending on the drawing history these samples reveal the so-called two- or four-point meridional scattering patterns. The intensity maxima are located on meridional layer lines which are parallel to the equator (see *Figure 4*). From the intensity distribution along the meridional layer line a lamellar structure with stacks of comparatively short crystalline lamellae, both perpendicular and inclined with respect to the drawing direction, was concluded[14].

With respect to the symmetry of the experimental scattering intensity, $I(b_r, b_3)$, the projection of $I(b_r, b_3)$ on to the b_3-axis is calculated according to equation (14). As a result, one-dimensional $I(b_3)$ curves, such as that shown for sample 9 in *Figure 5*, are obtained. These curves reveal an intensity maximum which corresponds to the average repeat distance along the b_3 axis and

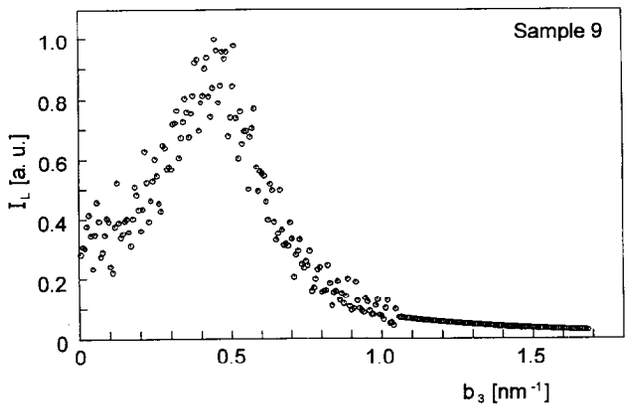

Figure 5 Projected one-dimensional scattering intensity curve, $I_L(b_3)$, of PET sample 9

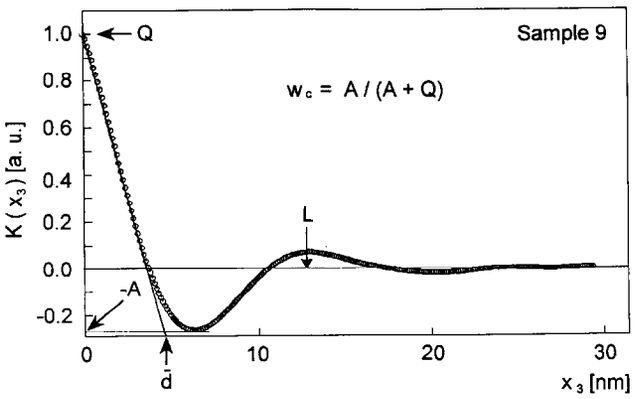

Figure 6 One-dimensional electron density correlation function, $K(x_3)$, of PET sample 9

Table 2 Structure parameters obtained from measurements with the Nicolet area detector

Sample	Most probable long period L (nm)	Average lamellar thickness $\bar{d}$ (nm)	Volume crystallinity w_c
2	15.0[a]	3.8	0.18
3	15.4	4.1	0.17
4	15.4	4.4	0.20
5	15.0	4.8	0.21
9	13.0	4.4	0.23

[a] Value is too large because of intensive equatorial scattering intensities

represents the sum of the crystalline and noncrystalline phase thicknesses along the drawing direction. As seen in *Figure 5*, the experimental SAXS curve is limited to a value of b_3 of $\sim 1.0\,\text{nm}^{-1}$. Because of the integration boundaries in equations (11) and (12) the projected $I_L(b_3)$ curve has to be extrapolated to $b_3 \rightarrow \infty$. This is achieved by means of Porod's law, according to equation (15). The extrapolated part of the $I_L(b_3)$ curve is also seen in *Figure 5*.

Using the projected scattering intensities in the interval from 0 to ∞ after extrapolation, the one-dimensional electron density correlation function, $K(x_3)$, is calculated according to equation (11). *Figure 6* represents the resulting function $K(x_3)$ for sample 9. As described above, such curves provide the most probable long period, L, the average lamellar thickness, $\bar{d}$, and the volume crystallinity, w_c. These parameters are presented in *Table 2* for both oriented and semicrystalline PET structures.

Depending on the drawing conditions, the structural parameters shown in *Table 2* do not appear to vary very much. The probable long period ranges from 13.0 to 15.4 nm, whereas the average lamellae thickness lies in the range between 3.8 and 4.8 nm and the volume crystallinity between 0.17 and 0.23. This small variance in the parameters is not surprising if we take into account the fact that all PET samples reveal an extremely large chain orientation. According to WAXS studies[17], the crystallites are almost perfectly aligned along the drawing direction. With respect to the second and fourth Legendre polynomials the orientation distribution should also be very narrow[17].

The values shown for the most probable long period in *Table 2* are large in comparison with those known from the literature for PET[8,19,20], which range from 7 to 18 nm. The chain anisotropy, as well as the crystallization conditions with regard to the crystalline/noncrystalline phase transition, affect the long period. Samples 2–5 were uniaxially drawn at very large stresses in the range from 350 to 400 MPa. As we are aware, such stresses are larger than those reported elsewhere. The thermal conditions during drawing, with temperatures from 160 to 230°C, together with these stress conditions, were responsible for the crystallization. From a comparison of the two-step drawn samples 5 and 9, with almost the same drawing temperature in the second step, the influence of the drawing stress on the draw ratio and the long period can be seen in *Tables 1* and *2*. The four-times-larger final drawing stress gave rise to a 1.33-times-larger draw ratio and consequently a larger long period for sample 5. The difference in the most probable long period of 2 nm between samples 5 and 9 is significant.

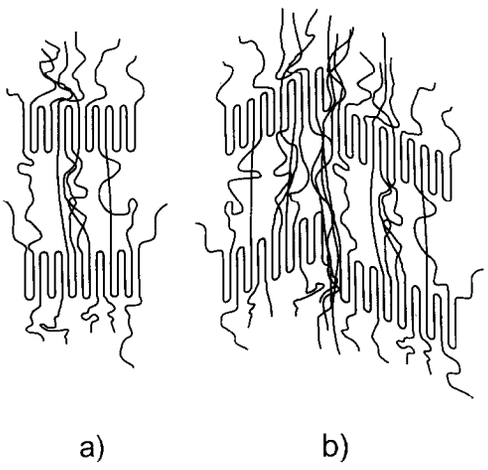

Figure 7 Structure models of uniaxially and highly oriented semicrystalline PET where the lamellae normal is parallel (a) and inclined (b) with respect to the drawing direction

In the case of sample 2 an intensive equatorial scattering is found which is most probably due to craze fibrils. These equatorial intensities superpose the intensity distribution along the meridional layer line (see *Figure 4*). Therefore, the long period determined from the correlation function is larger than the true value of the long spacing along the drawing direction (see *Table 2*).

Values for lamellar thickness, $\bar{d}$, are determined from the intersection of the extrapolated straight line, dK/dx_3, on the enveloped 'self-correlation triangle' at low x_3 values and the 'baseline' at $-A$. As seen in *Figure 3*, the 'baseline' which cuts the first $K(x_3)$ minimum belonging to the 'self-correlation-triangle' affects the $\bar{d}$ values very strongly. A comparison of the theoretical electron density correlation function, $K(x_3)$, in *Figure 2* with that obtained from the experimental results shown in *Figure 6* reveals differences in the regularity of the supermolecular structure. In accordance with Strobl and Schneider[6], $K(x_3)$ in *Figure 6* could be due to fluctuations in the interlamellar spacing, variations in the lamellar thickness, and diffuse phase boundaries. With respect to the correlation function there is a deviation from the idealized structure for all of the samples investigated. The average lamellar thickness values given in *Table 2* do not differ very greatly among the samples.

By using equation (13) with the parameters A and Q, the volume crystallinity can be determined. The largest crystallinity is obtained for sample 9, which was drawn at comparatively low stresses and temperature.

As seen in *Figure 4*, two- and four-point SAXS patterns are obtained for the uniaxially drawn PET samples. In accordance with our previous paper[14], two-point SAXS patterns are caused by lamellae stacks where the lamellae normal coincides with the drawing direction (see *Figure 7a*). In contrast to this, four-point SAXS patterns may be due to lamellae stacks where the lamellae normal is inclined with respect to the drawing direction (*Figure 7b*). These two structure models, shown in *Figure 7*, of uniaxially and highly oriented semicrystalline PET, are in agreement with the structural parameters determined from the electron density correlation function (see *Table 2*). The volume crystallinity of $\sim 20\%$ is only small and lets us suppose the existence of larger non-crystalline phases. The very large elastic moduli indicate a larger number of taut-tie molecules in the non-crystalline regions. A rough estimation of the amount of these molecules can be made by using a three-phase model, a crystallite modulus of $\sim 100\,\text{GPa}$[21,22], a modulus for the non-crystalline phase of $\sim 2\,\text{GPa}$[23], and the measured sample moduli, which ranges from 10 to 17 GPa.

CONCLUSIONS

Knowledge about the structure of crystalline and non-crystalline phases, and their spatial arrangement as well as phase boundaries, is of essential importance in understanding the structure–property relationships of semicrystalline polymers. In this present paper the supermolecular structure of uniaxially and highly oriented semicrystalline PET samples is discussed by applying the SAXS technique. Using the experimental two-dimensional scattering patterns, which includes structural information, the one-dimensional electron density correlation function is calculated in the case of cylindrical symmetry in the supermolecular structure. From the correlation function a most probable long period ranging from 13.0 to 15.4 nm, an average lamellae thickness between 3.8 and 4.8 nm, and a volume crystallinity between 0.17 and 0.23, are determined. On the basis of these parameters a structural model is established.

ACKNOWLEDGEMENT

The authors would like to thank Ch. Crook, I. Nanz, and T. Wagner for technical assistance.

REFERENCES

1 Glatter, O. and Kratky, O. 'Small Angle X-Ray Scattering', Academic, London, 1982
2 Feigin, L. A. and Svergun, D. I. 'Structure Analysis by Small-Angle X-Ray and Neutron Scattering', Plenum, New York, 1987
3 Alexander, L. E. 'X-Ray Diffraction Methods in Polymer Science', R. E. Krieger Publishing Company, Malabar, FL, 1969
4 Vonk, C. G. and Kortleve, G. *Kolloid-Z. Z. Polym.* 1967, **220,** 19
5 Kortleve, G. and Vonk, C. G. *Kolloid-Z. Z. Polym.* 1968, **225,** 124
6 Strobl, G. R. and Schneider, M. *J. Polym. Sci. Polym. Phys. Edn* 1980, **18,** 1343
7 Strobl, G. R., Schneider, M. and Voigt-Martin, I. G. *J. Polym. Sci. Polym. Phys. Edn* 1980, **18,** 1361
8 Santa Cruz, C., Stribeck, N., Zachmann, H. G. and Balta Calleja, F. J. Macromolecules 1991, **24,** 5980
9 Bonart, R. *Kolloid Z.-Z. Polym* 1966, **211,** 14
10 Dettenmaier, M. *Adv. Polym. Sci.* 1983, **52/53**
11 Stribeck, N. *Colloid Polym. Sci.* 1989, **267,** 301
12 Stribeck, N. *Colloid Polym. Sci.* 1992, **270,** 9
13 Stribeck, N., Apostolov, A. A., Zachmann, H. G., Fakirov, C., Stamm, M. and Fakirov, S. *Int. J. Polym. Mater.* 1994, **25,** 185
14 Göschel, U. *Polymer* 1995, **36,** 1157
15 Göschel, U. *Acta Polym.* 1989, **40,** 23

16 Hofmann, D., Göschel, U., Walenta, E., Geiß, D. and Philipp, B. *Polymer* 1989, **30,** 242
17 Göschel, U., Deutscher, K. and Abetz, V. *Polymer* in press
18 Porod, G. *Kolloid Z.* 1951, **124,** 83
19 Peszkin, P. N. and Schultz, J. M. *J. Polym. Sci. Polym. Phys. Edn* 1986, **24,** 2591
20 Groeninckx, G., Reynaers, H., Berghans, H. and Smets, G. *J. Polym. Sci. Polym. Phys. Edn* 1980, **18,** 1311
21 Dulmage, W. J. and Contois, L. E. *J. Polym. Sci.* 1958, **28,** 275
22 Sakurada, I., Ito, I. and Nakama, K. *J. Polym. Sci. (Part C)* 1966, **15,** 75
23 Göschel, U. and Nitzsche, K. *Acta Polym.* 1985, **36,** 580